A&A 505, 1041–1048 (2009)
DOI: 10.1051/0004-6361/200912118

Astronomy & Astrophysics

Wide and deep near-UV (360 nm) galaxy counts and the extragalactic background light with the Large Binocular Camera

A. Grazian[1], N. Menci[1], E. Giallongo[1], S. Gallozzi[1], F. Fontanot[2,3], A. Fontana[1], V. Testa[1], R. Ragazzoni[4], A. Baruffolo[4], G. Beccari[5], E. Diolaiti[6], A. Di Paola[1], J. Farinato[4], F. Gasparo[2], G. Gentile[4], R. Green[7], J. Hill[7], O. Kuhn[7], F. Pasian[2], F. Pedichini[1], M. Radovich[8], R. Smareglia[2], R. Speziali[1], D. Thompson[7], and R. M. Wagner[7]

[1] INAF – Osservatorio Astronomico di Roma, via Frascati 33, 00040 Monteporzio, Italy
e-mail: grazian@oa-roma.inaf.it
[2] INAF – Osservatorio Astronomico di Trieste, via G. B. Tiepolo 11, 34131 Trieste, Italy
[3] MPIA Max-Planck-Institute für Astronomie, Königstuhl 17, 69117 Heidelberg, Germany
[4] INAF – Osservatorio Astronomico di Padova, vicolo dell'Osservatorio 5, 35122 Padova, Italy
[5] ESA, Space Science Department, 2200 AG Noordwijk, The Netherlands
[6] INAF – Osservatorio Astronomico di Bologna, via Ranzani 1, 40127 Bologna, Italy
[7] Large Binocular Telescope Observatory, University of Arizona, 933 N. Cherry Ave., Tucson, AZ 85721-0065, USA
[8] INAF – Osservatorio Astronomico di Capodimonte, via Moiariello 16, 80131 Napoli, Italy

Received 19 March 2009 / Accepted 15 June 2009

ABSTRACT

Context. Deep multicolour surveys are the main tool for exploring the formation and evolution of the very faint galaxies that are beyond the spectroscopic limit of present technology. The photometric properties of these faint galaxies are usually compared with current renditions of semianalytical models to provide constraints on the detailed treatment of the fundamental physical processes involved in galaxy formation and evolution, namely the mass assembly and the star formation.
Aims. Galaxy counts over large sky areas in the 360 nm near-UV band are particularly difficult to obtain given the low efficiency of near-UV instrumentation, even at 8 m class telescopes. Observing in the near-UV bands can provide a first assessment of the distribution of star formation activity in distant (up to $z \sim 3$) galaxies. A relatively large instrumental field of view helps to minimize the biases caused by cosmic variance.
Methods. We obtained deep images in the 360 nm U band provided by the blue channel of the Large Binocular Camera at the prime focus of the Large Binocular Telescope. Over an area of ≃0.4 sq. deg., we derived the galaxy number counts down to $U = 27$ in the Vega system (corresponding to $U = 27.86$ in the AB system) at a completeness level of 30% reaching the faintest current limit for this wavelength and sky area.
Results. The shape of the galaxy number counts in the U band can be described by a double power-law, the bright side being consistent with the shape of shallower surveys of comparable or greater areas. The slope bends over significantly at $U > 23.5$ ensuring the convergence of the contribution by star-forming galaxies to the extragalactic background light in the near-UV band to a value that is more than 70% of the most recent upper limits derived for this band. We jointly compared our near-UV and K band counts collected from the literature with a few selected hierarchical CDM models, concentrating on specific critical issues in the physical description of the galaxy formation and evolution.

Key words. surveys – techniques: image processing – galaxies: photometry – galaxies: statistics

1. Introduction

Wide and deep multicolour surveys are useful tools for investigating in detail the processes of galaxy formation and evolution, especially beyond the spectroscopic capabilities of current instrumentation. One of the main aims of these deep multicolour surveys is to provide a clear picture of the processes involved in the mass assembly and star formation of galaxies across cosmic time. Galaxy observables, such as luminosity and mass functions, and two-point correlation function, are typically compared with current renditions of semi-analytical models in hierarchical CDM scenarios, to determine the key ingredients for an accurate description of the physics of galaxy formation (Croton et al. 2006; Menci et al. 2006; Bower et al. 2006; Nagamine et al. 2006; Fontanot et al. 2007; De Lucia & Blaizot 2007; Somerville et al. 2008; Keres et al. 2009; Dekel et al. 2009).

The observed properties of the galaxy population, however, are affected mainly by the limited statistics. Deep pencil beam surveys, such as GOODS (Giavalisco et al. 2004) or HUDF (Beckwith et al. 2003), have been carried out on relatively small sky areas and are affected significantly by cosmic variance. Larger surveys such as COSMOS, which extends over a 2 deg^2 area, are indeed shallower and limit the knowledge of the faint galaxy population at intermediate and high redshifts.

To probe the statistical properties of the faint galaxy population and reduce the biases due to the cosmic variance, a major imaging campaign should be performed over large areas with

efficient multicolour imagers at 8 m class telescopes. This is especially true in the near-UV band (hereafter UV), where instrumentation is in general less efficient but where it is possible to extract information about the star formation activity and dust absorption present in distant galaxies.

In this context, we are exploiting the unique power of the Large Binocular Camera (LBC) installed at the prime focus of the Large Binocular Telescope (LBT, Pedichini et al. 2003; Speziali et al. 2004; Ragazzoni et al. 2006; Hill et al. 2008; Giallongo et al. 2008) to reach faint magnitude limits in the U band ($\lambda \sim 3600$ Å) over areas of several hundreds of sq. arcmin.

Long LBC observations in the UV band are of comparable depth to those of the HDFs (although, obviously, the image quality is poorer). Even a single pointing with LBC produces a field two orders of magnitude larger than that of the combined HDF-N and HDF-S. This is very important because the transverse extent of the HDFs corresponds to about 1 Mpc at $z \sim 0.5-2$ where dark matter clustering is still important.

The goal of this paper is to provide UV (360 nm) galaxy number counts to the faintest magnitude limits available from ground-based observations. The comparison of both the normalization and shape of the observed counts with that predicted by theoretical hierarchical models can help to constrain the descriptions of galaxy formation and evolution, such as dust extinction and the formation of dwarf galaxies.

Throughout this paper, we adopt the Vega magnitude system ($U_{\rm Vega} = U_{\rm AB} - 0.86$) and we refer to differential number counts as simply "number counts", unless otherwise stated.

2. The data

The deep UV observations described here were carried out with the Large Binocular Camera (LBC, Giallongo et al. 2008), a double imager installed at the prime foci stations of the 8.4 m telescopes LBT (Large Binocular Telescope, Hill et al. 2008). Each LBT telescope unit is equipped with similar prime focus cameras. The blue channel (LBC-Blue) is optimized for imaging in the UV-B bands and the red channel (LBC-Red) for imaging in the VRIZY bands. The unvignetted FoV of each camera is 27 arcmin in diameter, and the detector area is equivalent to a 23×23 arcmin^2 field, covered by four 4 K by 2 K chips of pixel scale 0.225 arcsec. Because the mirrors of both channels are mounted on the same pointing system, a given target can be observed simultaneously over a wide wavelength range, improving the operation efficiency. Extensive descriptions of the twin LBC instrument can be found in Giallongo et al. (2008); Ragazzoni et al. (2006); Pedichini et al. (2003), and Speziali et al. (2008).

We used a deep U-BESSEL image of 3 hours, acquired in normal seeing conditions ($FWHM = 1$ arcsec) during the commissioning of the LBC-Blue camera, to derive faint UV galaxy-counts in a 478.2 arcmin^2 sky area to a faintness limit of U(Vega) = 26.5, in the Q0933+28 field (Steidel et al. 2003). The data were reduced using the LBC pipeline described in detail in Giallongo et al. (2008), applying the standard debias, flat-fielding, and stacking procedures to derive the coadded image. The flux calibration of the U-BESSEL image was derived by using observations of photometric standards from the fields SA98 and SA113 (Landolt et al. 1992) and the photometric fields of Galadi-Enriquez et al. (2000), as described in detail in Giallongo et al. (2008). The precision of the zeropoint calibration in the U-BESSEL filter is typically of the order of 0.03 mag at 68% confidence level. A correction to the photometric zeropoint of 0.11 mag due to the Galactic extinction was applied to the final coadd U-BESSEL image.

The Q0933+28 field was also imaged in the SDT-Uspec[1] filter of LBC for an additional hour in the first quarter of 2007, in normal seeing conditions (1.1 arcsec). These images are reduced and coadded in the same way as the U-BESSEL ones, except for the photometric calibration procedure, which is carried out using a spectrophotometric standard star of Oke (1990). The precision of the zeropoint calibration in the SDT-Uspec filter is typically of the order of 0.05 mag at 68% c.l. A Galactic extinction correction of 0.13 was used for this image.

To analyze the galaxy number counts deeper in the UV band, we coadded the image obtained in the U-BESSEL filter (with exposure time of 3 h) with this new one, after rescaling the two images to the same zeropoint. We verified that the effective wavelengths of these two filters are the same, the only difference being the higher transmission efficiency (1.5 times, after integrating its efficiency curve from $\lambda = 3000$ to 4000 Å) of the SDT-Uspec filter compared to the U-BESSEL one. The colour term between these two filters is 0.01, which we thus neglect when summing up the two images. The resulting image goes ~0.5 mag deeper than the original 3 h with U-BESSEL filter, given the higher image quality of the new SDT-Uspec image due to the general improvement of the telescope-instrument system, in particular the reduction of scattered light from the telescope and dome environment after the first run of the LBC-Blue commissioning. We use this final coadded image to improve the magnitude limit in the UV band and extend the number counts in this band to faint fluxes.

To decrease the effects of cosmic variance in the number counts at $U \sim 20$, we used 3 additional LBC fields with shallower magnitude limits $U \leq 25$ but of much larger area (892 arcmin^2) in the Subaru XMM Deep Survey (SXDS, Sekiguchi et al. 2004) region. These images were reduced and calibrated as described above for the Q0933+28 field. The $FWHM$ of these images (SXDS1, SXDS2, SXDS3) is higher (1.2, 1.25, 1.4 arcsec) than the one in the Q0933+28 field and the exposure time per LBC pointing is 1.0, 1.5, and 1.5 h, respectively, in the U-BESSEL filter. These three LBC images, combined with the deep point in the Q0933+28, field are then used to derive wide and deep galaxy number counts in the U band, from $U = 19.5$ to 25.0 over a FoV of 1370 arcmin^2 (0.38 sq. deg.) and to $U = 27.0$ for a subsample of ~480 arcmin^2.

3. The number counts in the *U* band

3.1. Deep U-band galaxy number counts

We computed galaxy number counts using the SExtractor package (Bertin & Arnouts 1996). For objects of area greater than that corresponding to a circular aperture of radius equal to the $FWHM$, we used the "best" photometry (Kron magnitude or corrected isophotal magnitude, if the galaxy is severely blended with surrounding objects) provided by SExtractor. For smaller sources, we computed magnitudes in circular apertures of diameter equal to 2 times the $FWHM$, and corrected them with an aperture correction that we derived using relatively bright stars in the field. This allows us to avoid the well known underestimate of the flux of faint galaxies provided by the isophotal method. To isolate the few stars from the numerous faint galaxies in this field, we relied on the class_star classifier provided by SExtractor. It is known that the morphological star/galaxy

[1] This is an interference filter with a wavelength range similar to a U-BESSEL filter, but the peak transmission is ~30% more efficient than that filter, as described in Fig. 2 of Giallongo et al. (2008).

classifier of SExtractor is not reliable for faint objects, but according to the model of Bahcall & Soneira (1980) the contamination from stars at faint U band fluxes and at high galactic latitude is very limited (1%). At brighter magnitudes, $U \sim 20$, the contamination from stars cannot be neglected, but at high S/N ratio, the morphological classification of SExtractor is robust. Moreover, the agreement between the LBC number counts at $U \leq 22$ and those of both SDSS and other large area surveys (e.g., VVDS) indicates that the contamination from Galactic stars is also lower for brighter U band magnitudes.

We search for an optimal configuration of SExtractor detection parameters to maximize the completeness at faint magnitude limits and reduce the number of unreliable detections. The two parameters regulating the depth, completeness, and reliability of the photometric catalog are the threshold (relative to the rms of the image) adopted for detection of objects and the minimum area of connected pixels above this threshold. We used the negative image technique, described in Dickinson et al. (2004); Yan & Windhorst (2004) and Bouwens et al. (2007), as an estimate of the reliability of the catalog. Using SExtractor, we produce the "-OBJECTS" image, i.e., the image with the detected objects subtracted, and then compute the negative of this image and run SExtractor with the same detection parameters used for the positive image. The sources detected on the negative image provide an estimate of the contamination from spurious sources, provided that the noise statistic is symmetric (towards positive and negative pixel values) in the image.

After several tests with different parameter sets, the most suitable combination are thresh = 0.7, and area = 8 pixels for Q0933+28 field, and thresh = 0.8, and area = 9 for SXDS fields (where the seeing is a bit worse), which minimize the number of spurious sources (measured in the negative image), while ensuring that the number counts and completeness of true sources remain relatively high at faint magnitude limits ($U \sim 26.5$). In the Q0933+28 field, the contamination from spurious sources is ~2.2% at $U = 26.5$, and remains lower than 2.5% to $U = 27.0$ (corresponding to U(AB) = 27.9).

The results of the galaxy number count analysis can be affected by the blending of galaxies when deep fields are investigated. In SExtractor, the two parameters affecting the deblending of sources are the DEBLEND_NTHRESH and DEBLEND_MINCONT parameters. We produce different catalogs using various combination of these two parameters for each LBC image, and we find that the raw number counts are insensitive to these parameters, since the number of galaxies per magnitude bin and per square degree varies between $\Delta\mathrm{Log}\,N = 0.02$ at $U = 24$–25 and $\Delta\mathrm{Log}\,N = 0.04$ at $U = 27$, our faintest bin in the galaxy number counts. We adopt DEBLEND_NTHRESH = 32 and DEBLEND_MINCONT = 0.002 for all the fields described here, based on visual inspection of the reliability of deblended sources on the Q0933+28 field.

The resulting raw counts are shown in Fig. 1, where a clear decrease is apparent for U(Vega) > 26.4. The typical photometric error at $U \sim 27$ is $\sigma = 0.4$ magnitudes, corresponding to a total integrated number count of ~100 galaxies per arcmin^2. An estimate of the completeness level should be performed to evaluate the amount of correction to the raw counts at the faint limits. This was evaluated by including in the true image 1000 simulated galaxies per 0.25 mag bin in the magnitude interval U(Vega) = 24–28 using the standard "artdata" package in IRAF. We included disk galaxies of half light radius 0.2–0.4 arcsec, convolved with the PSF of stellar objects in the field. We then run SExtractor on this new image using the same detection parameters described above, and determined how effective SExtractor

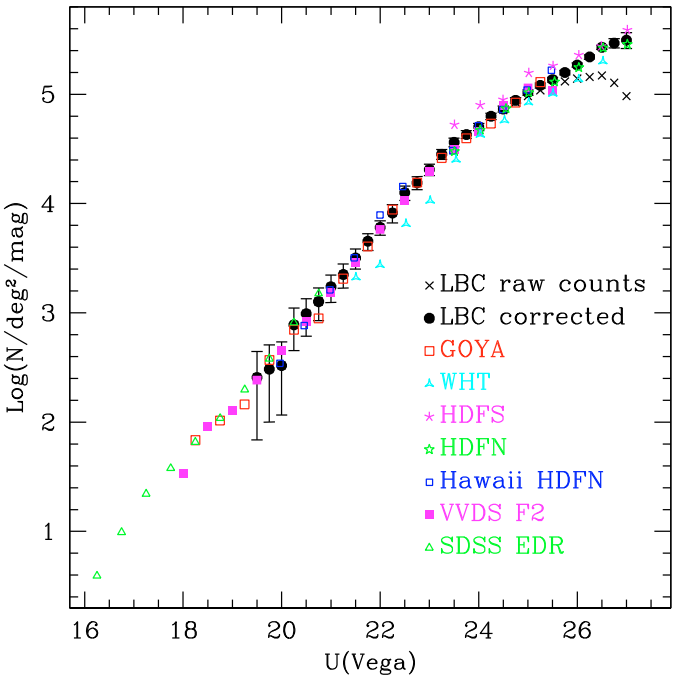

Fig. 1. Number counts of galaxies in the U-BESSEL band for the Q0933+28 and SXDS LBC fields. Black crosses represent the raw galaxy number counts, while filled big circles show the number counts corrected for incompleteness. Magnitudes are in the Vega system. We compare our counts with shallow surveys of similar or larger area (SDSS EDR, GOYA, VVDS F2), and with deeper pencil beam surveys (Hawaii HDFN, WHT, HDFN, HDFS).

is in recovering the simulated galaxies as a function of magnitude. The resulting sizes of the simulated galaxies are typical of real galaxies in the magnitude interval U(Vega) = 24–25, so the completeness that we computed at $U = 26$–27 can be considered to be a robust estimate. Using different datasets, i.e., Windhorst et al. (2002) and GOODS-South Grazian et al. (2006), we verified that, at $B \geq 25$, the half light radius of these galaxies is always between 0.2 and 0.4 arcsec. We choose not to use real sources to simulate the completeness of the images mainly for two reasons: the half light radii of galaxies decrease with magnitude, and it is known that fainter galaxies are smaller. If we use bright ($U \leq 24$) high signal-to-noise objects, their size, once dimmed to $U \sim 26$–27, can be overestimated with respect to their true size, enhancing artificially the completeness correction at fainter magnitudes. If we use real faint sources as input in our simulations, the signal-to-noise ratio of these galaxies is very low, enhancing even in this case the completeness correction. We tried instead a robust and realistic assumption, which is to simulate galaxies with half light radius between 0.2 and 0.4 arcsec, the range observed at faint magnitude limits where morphological analysis is still reliable (see e.g. Conselice et al. 2008). The completeness at $U \leq 25.5$ does not depend on the half light radius of the simulated galaxies, while at fainter magnitudes it does depend on the galaxy size: in particular, at $U = 26.0$ the scatter in the completeness for various half light radii between 0.2 and 0.4 arcsec is 3%, increasing to 6% at $U = 26.5$, and reaching 16% at $U = 27.0$. The resulting 50% completeness level is measured at U(Vega) = 26.6, while at $U = 27.0$ we have a formal completeness of 30%.

The number counts corrected for incompleteness are shown in Fig. 1. Given the wide magnitude interval from U(Vega) = 19.5 to U(Vega) = 27.0 available in the present survey, the shape

of the count distribution can be derived from a single survey in a self-consistent way, possibly minimizing offsets due to systematics in the photometric analysis of data from multiple surveys (zeropoint calibration, and field-to-field variation). A clear bending is apparent at $U(\mathrm{Vega}) > 23.5$. To quantify the effect, we fitted the shape of the counts in the above magnitude interval with a double power-law. The slope changes from 0.58 ± 0.03 to 0.24 ± 0.05 for magnitudes fainter than $U_{\mathrm{break}} = 23.6$. The uncertainty in the break magnitude is however large, ~0.5, since the transition between the two regimes of the number counts is gradual.

In Fig. 1, we compare our galaxy number counts with those derived by shallow surveys of large area (SDSS EDR, Yasuda et al. 2001) or of similar area (GOYA by Eliche-Moral et al. 2006; VVDS-F2 by Radovich et al. 2004), and with deep pencil beam surveys (Hawaii HDFN by Capak et al. 2004; WHT, HDFN, and HDFS by Metcalfe et al. 2001). In particular, the WHT galaxy counts (Metcalfe et al. 2001) are based on a 34 h exposure time image reaching $U(\mathrm{Vega}) = 26.8$ but at the much lower 3σ level in the photometric noise and in an area of ~50 arcmin^2, while the GOYA survey at the INT telescope is complete at the 50% level at $U(\mathrm{Vega}) = 24.8$. These counts are shown together with the two pencil beam surveys in the Hubble Deep Fields (Metcalfe et al. 2001). The agreement with the GOYA survey (900 sq. arcmin.) is remarkable, and suggests that once big areas of the sky are investigated, the effects of cosmic variance are slightly reduced. The present UV counts obtained during the commissioning of LBC-Blue are thus a unique combination of deep imaging in the U band and of large sky area, resulting in considerable reduction in the cosmic variance effects for $U \geq 21$. For brighter magnitude limits, we refer to larger area surveys, shallower than our survey, as shown in Fig. 1.

Table 1 summarizes the galaxy number counts, corrected for incompleteness, with their upper and lower 1σ confidence level uncertainties, assuming Poisson noise and the cosmic variance effect. For the latter, we used the cosmic variance calculator (v1.02) developed by Trenti & Stiavelli (2008) using as input values a linear size of 22 arcmin (corresponding to our deeper area of 478.2 arcmin^2) and redshift from 0.0 to 3.0, for a standard Λ-CDM cosmology. At $U = 27$, for example, the computed cosmic variance is 4.5%.

Using the Q0933+28 and the three fields in the SXDS area, we study the field to field variation in the number counts in the U band. We find that the typical variation from one LBC field to another is 0.04 in Log N for $U \sim 20$, while it reduces gradually to 0.01 at $U = 24.5$, well below the Poissonian uncertainties described in Table 1. This ensures that the zeropoint calibration of the images is robust and the area of this survey is sufficient to decrease the cosmic variance effects below the statistical uncertainties in the galaxy number counts. We complement these internal checks on the galaxy number counts in U with an external consistency test, comparing our final number counts with shallower ones derived in different areas or deep pencil beam surveys in Fig. 1. We find that the survey-to-survey maximal variations are of the order of 0.1 in Log N at all magnitudes, with lower scatter for the wider surveys considered here (GOYA, SDSS-EDR, VVDS-F2).

3.2. The UV extragalactic background light

The slope of the galaxy number counts in the U band at $U \sim 23.5$ changes from 0.58 to 0.24, which implies that the contribution of galaxies to the integrated EBL in the UV has a maximum around this magnitude. The contribution of observed galaxies to the optical extragalactic background light (EBL) in the UV band can be computed directly by integrating the emitted flux multiplied by the differential number counts down to the completeness limit of the survey.

Table 1. LBC U galaxy number counts.

U(Vega)	Log N	Max Log N	Min Log N	Completeness
19.50	2.409	2.648	1.837	1.00
19.75	2.484	2.707	2.001	1.00
20.00	2.517	2.734	2.066	1.00
20.25	2.891	3.043	2.654	1.00
20.50	2.991	3.129	2.787	1.00
20.75	3.103	3.227	2.930	1.00
21.00	3.239	3.346	3.095	1.00
21.25	3.350	3.446	3.227	1.00
21.50	3.503	3.585	3.401	1.00
21.75	3.655	3.725	3.572	1.00
22.00	3.782	3.843	3.711	1.00
22.25	3.914	3.989	3.824	1.00
22.50	4.100	4.161	4.028	1.00
22.75	4.191	4.247	4.127	1.00
23.00	4.311	4.360	4.256	1.00
23.25	4.452	4.494	4.405	1.00
23.50	4.561	4.598	4.521	1.00
23.75	4.633	4.667	4.595	1.00
24.00	4.702	4.734	4.668	1.00
24.25	4.799	4.827	4.768	0.99
24.50	4.865	4.892	4.837	0.98
24.75	4.945	4.970	4.919	0.96
25.00	5.016	5.040	4.992	0.93
25.25	5.081	5.103	5.058	0.90
25.50	5.135	5.156	5.113	0.88
25.75	5.199	5.219	5.178	0.83
26.00	5.268	5.288	5.248	0.75
26.25	5.341	5.361	5.321	0.66
26.50	5.431	5.450	5.411	0.55
26.75	5.469	5.510	5.425	0.43
27.00	5.495	5.563	5.419	0.30

LBC U galaxy number counts corrected for incompleteness; N is the number of galaxies per deg^2 and per magnitude bin, while the minimum and maximum counts are the 1σ confidence level (Poisson noise and cosmic variance effect).

Following the work of Madau & Pozzetti (2000), we compute the EBL in the U band, I_ν measured in erg s^{-1} cm^{-2} Hz^{-1} Sr^{-1}, using the method

$$I_\nu = 10^{-0.4(U_{\mathrm{AB}}+48.6)} N(U_{\mathrm{AB}}), \quad (1)$$

where we use the following correction from Vega to AB: $U_{\mathrm{AB}} = U_{\mathrm{Vega}} + 0.86$.

Figure 2 shows the EBL obtained by the LBC deep number counts and compares it with the results of Madau & Pozzetti (2000). Our data agrees well with previous estimates of the EBL in the U band, and indeed it allows us to derive precisely the peak of the differential EBL, at $U = 23.55 \pm 0.25$, and place strong constraints on the contributions of faint galaxies to $U = 27.0$ to the integrated EBL in this band. At magnitudes $U \geq 24$, our estimate of the EBL is significantly higher than the one of Madau & Pozzetti (2000). Checking Fig. 1 in detail, it is clear that the HDFS is slightly underdense with respect to the HDFN or other deep pencil beam surveys, probably because of cosmic variance effects, and this is reflected in the lower EBL of Madau & Pozzetti (2000) compared to the LBC estimate.

The integrated galaxy contribution to the EBL in the UV band implies that $\nu I(\nu) = 3.428 \pm 0.068$ nW/m^2/Sr at the effective wavelength of the LBC U-BESSEL filter, 3590 Å, taking

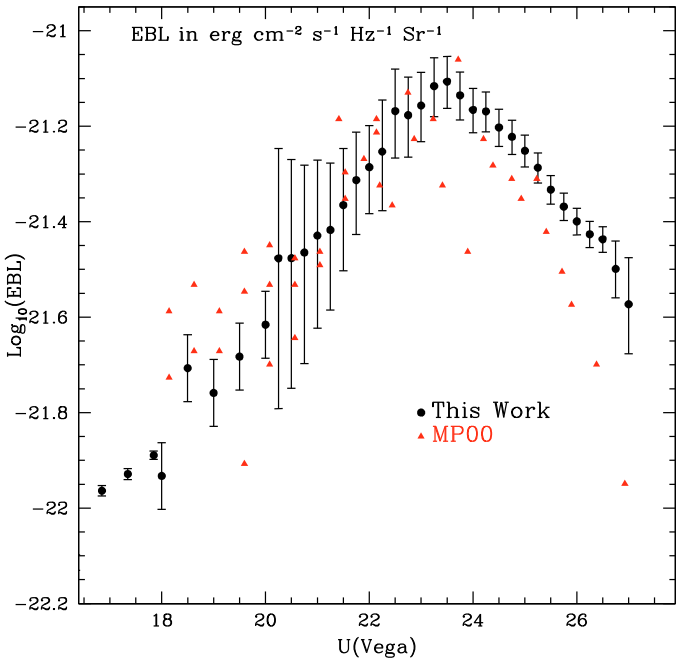

Fig. 2. The extragalactic background light per magnitude bin I_ν as a function of U band magnitudes. We compare the results of this work with the EBL derived by Madau & Pozzetti (2000) in the HDFS field. The small error bars of EBL at $U \leq 18$ are due to the small uncertainties in the galaxy number counts derived using SDSS data.

into account the magnitude range $U = 17$–27. This estimate is 20% higher than the one estimated by Madau & Pozzetti (2000) ($2.87^{+0.58}_{-0.42}$ nW/m^2/Sr), although their value is still consistent with our measurement due to their large uncertainties. Moreover, our estimate reduces the uncertainties by an order of magnitudes, which is of fundamental importance to placing strong constraints on galaxy evolution models. Extrapolating the observed number counts in the U band down to flux = 0, we derive an integrated EBL of $\nu I(\nu) = 3.727 \pm 0.084$ nW/m^2/Sr, i.e., in our survey to $U = 27$ we resolve 92% of the EBL produced by galaxies.

The integrated flux from resolved galaxies, however, should be considered as a lower limit to the total EBL in the universe, since our estimate could be affected by different systematics:

- incompleteness in the number counts at faint magnitudes caused by the presence of very extended/diffuse sources that escape detection in our LBC deep images and in the HDFs surveys. The adopted detection algorithms usually select galaxies down to a threshold in their surface brightness limits, and so are prone to selection effects against low surface brightness galaxies. We computed the completeness of galaxies assuming a conservative half light radius of 0.3 arcsec, and we cannot exclude the presence of a population of diffuse and extended galaxies in the UV bands, even this hypothesis is quite unlikely, because of the well known relation between observed optical magnitudes and half light radius of galaxies (Totani et al. 2001);
- the surface brightness dimming of sources at high redshifts. This is not a serious problem in the U band, since all the light in this wavelengths originates from $z \leq 3$ galaxies (non U-dropout galaxies) and, as discussed in the next paragraph, the redshift distribution of galaxies contributing to the peak of the EBL are at $z \leq 1$.

Independent estimates to the total EBL in the U band are given in Bernstein et al. (2002) and Bernstein (2007), and are slightly higher than our estimate from the galaxy number counts: $\nu I(\nu) = 14.4 \pm 9$ nW/m^2/Sr in Bernstein et al. (2002) and $\nu I(\nu) = 21.6 \pm 14.4$ nW/m^2/Sr in Bernstein (2007), after a different treatment for the contaminating foregrounds.

With the present observations, we reject the hypothesis of Bernstein et al. (2002) that an enormous contribution to the sky background in the U band is made by the overlapping wings of extended galaxies. With the present observations, we reach a surface brightness limit of $U = 28.2$ mag/arcsec^2 at 3σ and thus exclude the presence of faint and extended wings in the galaxy UV light distributions.

The discrepancy between the resolved and total EBL could be explained by a population of ultra faint and numerous galaxies at $U \geq 27$, beyond the current limits of the present surveys and with a $\log N$–$\log S$ slope steeper than 0.5, or by an improper subtraction of the foreground components, as stated in Mattila (2003) and Bernstein (2007).

Recently, Georganopoulos et al. (2008) proposed a new method to derive stringent limits to the diffuse light in the UV bands, by measuring the inverse Compton emission in γ-rays of the EBL by the high energy electrons in the radio lobes of Fornax A. This technique will allow to derive constraints to the EBL at shorter wavelengths than the limits obtained by the TeV blazar emission (Stanev & Franceschini 1998; Aharonian et al. 2006; Albert et al. 2008). At the present stage, Albert et al. (2008) give an upper limit of $\nu I(\nu) \leq 5$ nW/m^2/Sr to the total EBL in the UV. This limit strengthens the hypothesis that the discrepancy between our estimate of the EBL in U band and that of Bernstein (2007) is due to a foreground local component.

Our derivation of the EBL by integrated galaxy counts is marginally consistent with the lower limit derived by Kneiske & Dole (2008) of $\nu I(\nu) \geq 3.97$ nW/m^2/Sr at $\lambda = 3600$ Å.

4. Comparison with theoretical models

The availability of galaxy number counts to faint magnitude limits and over large sky areas can be used to test the predictions of different theoretical models without being strongly affected by cosmic variance. Among the various models (numerical and semi-analytical) developed in the framework of the standard hierarchical CDM scenario, we selected the models developed by Menci et al. (2006, hereafter M06), the Kitzbichler & White (2007) model based on the Millennium Simulation (hereafter K07), and the model developed by Monaco et al. (2007, hereafter MORGANA). All these models simulate the formation and evolution of galaxies, starting from a statistical description of the evolution of the DM halo population (merger trees), and using a set of approximated, though physically motivated, "recipes" to treat the physical processes (gas cooling, star formation, AGN and SF feedback, stellar population synthesis) acting on the baryonic component. An appropriate treatment of dust attenuation is also important when comparing model predictions to the UV observations, given the efficient scattering of radiation at these wavelengths by dust grains, as shown by the GALEX number counts of Xu et al. (2005).

The comparison of the observed counts with that predicted by the three selected models is used to enlighten different critical issues concerning the physical description of the galaxy formation and evolution.

In particular, the M06 model is characterized by a specific implementation of the AGN feedback on the star formation activity in high redshift galaxies. The description is based on the

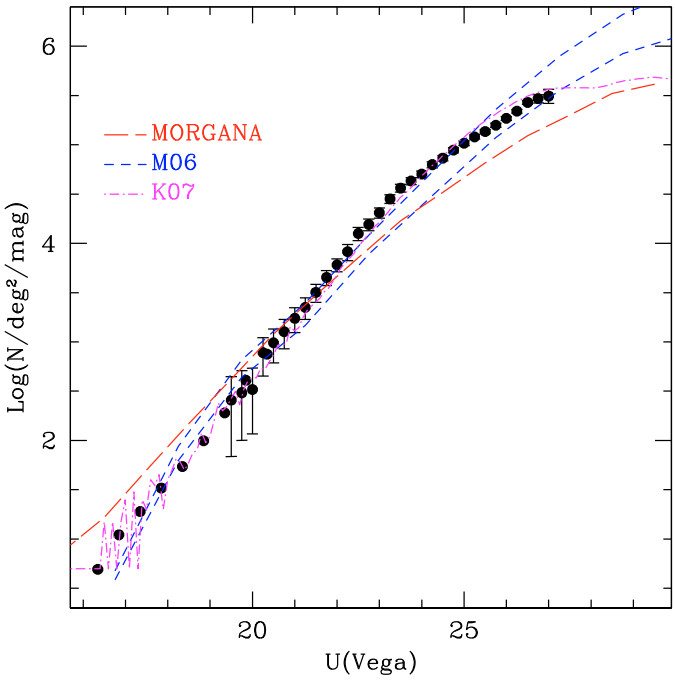

Fig. 3. Number counts of galaxies in the U-BESSEL band for the Q0933+28 LBC field, complemented at brighter magnitudes ($U \leq 20$) by the number counts of VVDS-F2 and SDSS-EDR, whose error bars are always smaller than the size of the points. We compare our counts with theoretical models (M06, K07, MORGANA).

expanding blast waves as a mechanism for propagating outwards the AGN energy injected into the interstellar medium at the centre of galaxies (see Menci et al. 2008); such a feedback is only active during the active AGN phase ("QSO mode"), and it is effective in suppressing the star formation in massive galaxies already by $z \approx 2$, thus yielding a fraction of massive and extremely-red objects in approximate agreement with observations (Menci et al. 2006). The M06 model uses three different prescriptions for the dust absorption, namely the Small Magellanic Cloud model (SMC), the Milky Way (MW) law, and the Calzetti et al. (2000) extinction curve (C00). In Fig. 3, the two short-dashed curves enclose the minimum and maximum number counts predicted by the M06 model, taking into account the three different extinction curves (SMC, MW, and C00).

The model of Kitzbichler & White (2007) is based on the Millennium Simulation (Springel et al. 2005) and a concordance Lambda CDM cosmology. In the model, the particle mass resolution of the code can affect the physical and statistical properties of faint low-luminosity galaxies. The adopted CDM mass resolution is sufficient to resolve a halo hosting a galaxy as faint as 0.1 L^* with at least 100 particles of $8.6 \times 10^8\ h^{-1}\ M_\odot$. The model also adopts a different AGN feedback called "radio mode" in which cooling is suppressed by the continuous accretion of hot gas onto supermassive black holes at the centre of groups or cluster of galaxies. The only difference between K07 and both Croton et al. (2006) and De Lucia & Blaizot (2007) is in the dust model used in their simulations. For the local galaxies, they adopt a simple relationship between face-on optical depth and intrinsic luminosity $\tau \propto \tau_0 (L/L_*)^\beta$ with $\beta = 0.5$. At high redshifts, they take into account the different dust and gas contents, the varying metallicities, and the shorter rest-frame emitted wavelengths. In particular, their average extinction increases significantly towards high redshifts because of the smaller disc sizes of the galaxies. We refer to Kitzbichler & White (2007) for details of their dust model.

Finally, the MORGANA model is characterized by a different treatment of the processes of gas cooling and infall (following Viola et al. 2008), star formation, and feedback (using the multi-phase model of Monaco 2004). Black hole accretion is described in detail in Fontanot et al. (2006): the accretion rate in Eddington units determines the nature of feedback from the AGN. Synthetic SEDs for model galaxies are obtained using the GRASIL code (Silva et al. 1998), which explicitly solves the equation of radiative transfer in a dusty medium. Fontanot et al. (2006) show that MORGANA is able to reproduce both sub-mm (850 μm) number counts and the redshift distribution observed in K-limited samples with a conservative choice of the stellar IMF. Galaxy SEDs, magnitudes, and colours for a variety of passbands are obtained using the GRASIL spectrophotometric code (Silva et al. 1998), which explicitely solves the equations for the radiative transfer in a dusty medium taking into account the composite geometry (bulge+disc) of each model galaxy. The dust properties (dust-to-gas mass fractions, composition, and size distribution) are kept fixed to values providing good agreement with local observations (see Fontanot et al. 2007, for more details about the coupling between MORGANA and GRASIL). In this work, we take advantage of updates to the model, which was adapted for a WMAP3 cosmology and Chabrier IMF as presented in Lo Faro et al. (2009).

It is worth noticing that photoelectric absorption by the interstellar medium is redshifted, for high redshift galaxies, into the observed UV band. For this reason, only galaxies with $z < 3$ contribute to the UV number counts. The common characteristics of the models is that only galaxies in the $1.5 < z < 2.5$ redshift intervals provide the main contribution to the counts at $U > 26$ (see Barro et al. 2009). This implies that the shape of the faint counts is provided by the average faint-end shape of the galaxy luminosity function in the same redshift interval.

The comparison of the observed galaxy number counts in the U (360 nm) band with the predictions of theoretical models shown in Fig. 3 indicates that:

- the M06 and K07 models reasonably reproduce the UV number counts from $U = 17$ to $U = 27$, while the MORGANA model exhibits the greatest disagreement with the observed data;
- the three models show different shapes for the UV galaxy number counts at faint fluxes, implying that discrepancies increase with increasing magnitudes. This can be evaluated in more detail by dividing the counts in redshift bins (see Barro et al. 2009);
- with the current observations of the UV number counts down to $U = 27$, both M06 and K07 models show similar behaviour, although the K07 model appears to curve over for $U > 27$ in contrast to the steeper slope of the M06 model.

The discrepancies between predicted and observed faint UV galaxy number counts could be due in principle to several effects, e.g., the evolution in number density, star formation activity, or dust extinction of the faint galaxy population. Among these, an appropriate treatment of the dust extinction plays an important role, in this comparison based on the U band, since it can affect both the normalization and shape of the observed UV counts. The effects caused by the different extinction laws (Calzetti 2000, and Small Magellanic Cloud) adopted in the M06 model for example, increase at fainter magnitudes since we are observing galaxies at high ($z < 3$) redshifts. In this respect, the

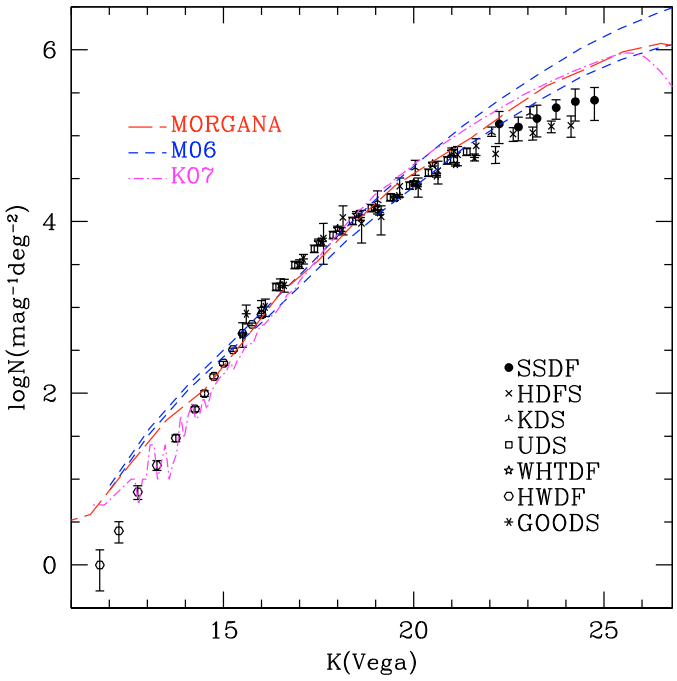

Fig. 4. Number counts of galaxies in the K band for different deep surveys in the literature. The model predictions come from the same models described in the previous figure.

curve observed in the UV counts could be indicative of a gradual redshift evolution in the dust properties.

Another physical quantity relevant to the correct reproduction of the faint counts is the amount of star formation activity in faint low-mass galaxies. This effect is particularly important in the MORGANA model, where it is responsible for the flat shape of the predicted counts. Fontanot et al. (2009) show that the underprediction of UV number counts of faint galaxies can be explained by a rapid decline in their star formation activity and consequently in their associated UV emission at $z \lesssim 2$. These galaxies are predicted to be too passive and to host too old stellar populations at later times with respect to observations. The reduced SFRs can easily explain the flat shape of the predicted counts in MORGANA.

As an attempt to disentangle dust/SFR effects from number density evolution, we extended the model comparison to the NIR K band number counts, which are much less sensitive to dust absorption and short episodes of star formation. The observed flux in the K band is more related to the star formation history in the galaxy quantified by its assembled stellar mass (see e.g., Fontana et al. 2006). Figure 4 compares observed number counts in the K band collected from the literature and provided by different instruments/telescopes and surveys (SSDF: Minowa et al. 2005; HDFS: Labbé et al. 2003; KDS: Moustakas et al. 1997; UDS: Cirasuolo et al. 2008; WHTDF: Cristobal-Hornillos et al. 2003; HWDF: Huang et al. 1997; GOODS: Grazian et al. 2006) with the model predictions of M06, K07, and MORGANA. The observed K band galaxy counts show a clear bend at $K \simeq 17$, where the average slope changes from 0.69 to a flatter value of 0.33. Here the bending is clearer than observed in the UV, since the break magnitude is brighter than the faintest survey limits.

In the K band, the models tend to overestimate the number counts both at the bright end $K < 15$ and at faint magnitudes $K > 20$. The excess in the predicted K band number counts resembles that at the faint end of the theoretical luminosity functions in the NIR (see for example Poli et al. 2003; and Fontanot et al. 2009). This can be indicative of an excess in the production of galaxies with low luminosity and high redshifts. If the NIR number counts are extrapolated to fainter limits, the amount of excess differs among the models, being smaller in the K07 model at $K \geq 26$. The latter however is affected by a threshold in the mass resolution used by the numerical code of the Millennium simulation adopted in the K07 model. This could provide an artificial removal of faint galaxies.

The simultaneous comparison of the UV and NIR K band number counts at faint fluxes seems to indicate that the underprediction of the modelled UV number counts could be caused by dust extinction or reduced SF activity rather than intrinsic evolution in the galaxy number density.

Finally, we identify a third problem when comparing the bright end of the galaxy counts, where the treatment of the feedback on SF processes due to AGN activity can play an important role. The M06 model for example shows the effect of a different treatment of AGN feedback based on the so-called QSO mode compared to the radio mode feedback used by the K07 model, while MORGANA is characterized by both the radio and QSO modes. The different treatment of AGN feedback is plausibly responsible for the differences in the predictions of NIR galaxy number counts at $K \leq 15$. The excess in the UV number counts predicted by models is related to the quenching of the star formation activity. MORGANA tends to overpredict star formation activity in massive central galaxies at low-z. This is related to the less efficient, or delayed, quenching of the cooling flows in massive halos by radio-mode feedback. In this model, gas accretion onto the central black hole is related to star formation activity in the spheroidal component: this implies that AGN heating switches on only after some cooled gas has already started forming stars in the host galaxy (see Kimm et al. 2008, for a complete discussion and a comparison of different radio-mode implementations in semi-analytical models).

As a last comment, all the three models include a contribution to the UV EBL that is broadly consistent with the upper limits described in Sect. 3.2. Using the same method described there for the observed data, we derived an EBL of 0.71–1.18 nW/m^2/Sr for the M06 model in the UV band, while the MORGANA and K07 model have 2.66 and 3.26 nW/m^2/Sr, respectively.

5. Summary

To summarize the main results of the paper:

- We have derived in a relatively wide field of 0.4 deg^2 the deepest counts published to date in the 360 nm UV band. This has allowed us to evaluate the shape of the galaxy number counts in a wide magnitude interval $U = 19$–27 with the advantage of mitigating cosmic variance effects. The agreement with the number counts of shallower surveys confirms the low impact of systematic errors on LBC galaxy statistics.
- The shape of the counts in UV can be described by a double power-law with a steep slope 0.58 followed beyond $U \simeq 23.5$ by a flatter shape 0.24. Our counts are consistent at the bright end with surveys of comparable or greater areas. At the faint end, our counts are more consistent with that found in the HDF-N.
- The faint-end slope of the counts is below 0.4 and this ensures the convergence of the contribution by star-forming galaxies to the EBL in the UV band. The total value in the UV band obtained by extrapolating the slope of our counts

to flux = 0 is indeed 3.727 ± 0.084 nW/m^2/Sr. It is consistent with upper limits derived from TeV observations of Albert et al. (2008), $\nu I(\nu) \leq 5$ nW/m^2/Sr, showing that the UV EBL is resolved at $\geq$74% level.

- We have compared our counts in the UV and K bands with the predictions of a few selected hierarchical CDM models considering different and important issues in the physical description of the galaxy formation and evolution.
- The mass resolution of numerical models is critical to reproducing the faint end of the UV galaxy number counts.
- The discrepancies between predicted and observed UV galaxy number counts at faint magnitudes could be mainly due to the treatment of dust extinction and the star formation activity in low mass galaxies at $z \leq 2$.
- The AGN feedback (radio versus QSO mode) may affect galaxy counts at the bright end of the $\log N$–$\log S$ in the K band.

A correct physical description of the AGN feedback, dust properties, and star formation activities in the models is fundamental to ensure reasonable agreement with the model predictions at the faint end of the galaxy counts.

Adding colour information for galaxies with UV emission as faint as $U = 27$–28 will require very deep observations in the red bands that are feasible with several hours of integration at 8 m class telescopes. Very deep multicolour information over areas of the order of a square degree can help in extracting physical information about the star formation history of the dwarf population at intermediate and high redshifts.

Acknowledgements. Observations have been carried out using the Large Binocular Telescope at Mt. Graham, Arizona, under the Commissioning phase of the Large Binocular Blue Camera. The LBT is an international collaboration among institutions in the United States, Italy and Germany. LBT Corporation partners are: the University of Arizona on behalf of the Arizona university system; Istituto Nazionale di Astrofisica, Italy; LBT Beteiligungsgesellschaft, Germany, representing the Max-Planck Society, the Astrophysical Institute Potsdam, and Heidelberg University; The Ohio State University, and The Research Corporation, on behalf of The University of Notre Dame, University of Minnesota and University of Virginia. The Millennium Simulation databases used in this paper and the web application providing online access to them were constructed as part of the activities of the German Astrophysical Virtual Observatory. Some of the calculations were carried out on the PIA cluster of the Max-Planck-Institut für Astronomie at the Rechenzentrum Garching. We thank the anonymous referee for useful comments which helps in improving the quality of the present paper. A.G. warmly thanks Kalevi Mattila and Martin Raue for useful comments on the EBL limits.

References

Aharonian, F., Akhperjanian, A. G., Bazer-Bachi, A. R., et al. 2006, Nature, 440, 1018
Albert, J., Aliu, E., Anderhub, H., et al. 2008, Science, 320, 1752
Bahcall, J. N., & Soneira, R. M. 1980, ApJS, 44, 73
Barro, G., Gallego, J., Pérez-González, P. G., et al. 2009, A&A, 494, 63
Beckwith, S. V. W., Caldwell, J., Clampin, M., et al. 2003, A&AS, 202, 1705
Bernstein, R. A. 2007, ApJ, 666, 663
Bernstein, R. A., Freedman, W. L., & Madore, B. F. 2002, ApJ, 571, 56
Bertin, E., & Arnouts, S. 1996, A&AS, 117, 393
Bower, R. G., Benson, A. J., Malbon, R., et al. 2006, MNRAS, 370, 645
Bouwens, R. J., Illingworth, G. D., Franx, M., & Ford, H. 2007, ApJ, 670, 928
Calzetti, D., Armus, L., Bohlin, R. C., et al. 2000, ApJ, 533, 682
Capak, P., Cowie, L. L., Hu, E. M., et al. 2004, AJ, 127, 180
Cirasuolo, M., McLure, R. J., Dunlop, J. S., et al. 2008, MNRAS, submitted, submitted, [arXiv:0804.3471]
Conselice, C. J., Rajgor, S., & Myers, R. 2008, MNRAS, 386, 909
Cristobal-Hornillos, D., Balcells, M., Prieto, M., et al. 2003, ApJ, 595, 71
Croton, D. J., Springel, V., White, S. D. M., et al. 2006, MNRAS, 365, 11
Dekel, A., Birnboim, Y., Engel, G., et al. 2009, Nature, 457, 451
De Lucia, G., & Blaizot, J. 2007, MNRAS, 375, 2
Dickinson, M., Stern, D., Giavalisco, M., et al. 2004, ApJ, 600, L99
Eliche-Moral, M. C., Balcells, M., Prieto, M., et al. 2006, ApJ, 639, 644
Fontana, A., Salimbeni, S., Grazian, A., et al. 2006, A&A, 459, 745
Fontanot, F., Monaco, P., Cristiani, S., & Tozzi, P. 2006, MNRAS, 373, 1173
Fontanot, F., Monaco, P., Silva, L., & Grazian, A. 2007, MNRAS, 382, 903
Fontanot, F., De Lucia, G., Monaco, P., Somerville, R. S., & Santini, P. 2009, MNRAS, 397, 1776
Galadi-Enriquez, D., Trullols, E., & Jordi, C. 2000, A&AS, 146, 169
Georganopoulos, M., Sambruna, R. M., Kazanas, D., et al. 2008, ApJ, 686, L5
Giallongo, E., Ragazzoni, R., Grazian, A., et al. 2008 A&A, 482, 349
Giavalisco, M., & the GOODS Team 2004, ApJ, 600, L93
Grazian, A., Fontana, A., De Santis, C., et al. 2006, A&A, 449, 951
Hill, J. M., Green, R. F., Slagle, J. H., et al. 2008, Proc. SPIE, 7012, 701203
Huang, J. S., Cowie,, L. L., Gardner, J. P., et al. 1997, ApJ, 476, 12
Keres, D., Katz, N., Dave, R., Fardal, M., & Weinberg, D. H. 2009, MNRAS, 396, 2332
Kimm, T., Somerville, R. S., Yi, S. K., et al. 2009, MNRAS, 394, 1131
Kitzbichler, M. G., & White, S. D. M. 2007, MNRAS, 376, 2
Kneiske, T. M., & Dole, H. 2008, High Energy Gamma-Ray Astronomy: 4th International Symposium, Proceedings of the conference held July 7–11, in Heidelberg, Germany
Labbé, I., Franx, M., Rudnick, G., et al. 2003, ApJ, 125, 1107
Landolt, A. U. 1992, AJ, 104, 372
Lo Faro, B., Monaco, P., Vanzella, E., et al. 2009, MNRAS, tmp 1225, [arXiv:0906.4998]
Madau, P., & Pozzetti, L. 2000, MNRAS, 312, L9
Mattila, K. 2003, ApJ, 591, 119
Menci, N., Fontana, A., Giallongo, E., Grazian, A., & Salimbeni, S. 2006, ApJ, 647, 753
Metcalfe, N., Shanks, T., Campos, A., McCracken, H. J., & Fong, R. 2001, MNRAS, 323, 795
Minowa, Y., Kobayashi, N., Yoshi, Y., et al. 2005, ApJ, 629, 29
Monaco, P. 2004, MNRAS, 352, 181
Monaco, P., Fontanot, F., & Taffoni, G. 2007, MNRAS, 375, 1189
Moustakas, L. A., Davis, M., Graham, J. R., et al. 1997, ApJ, 475, 445
Nagamine, K., Ostriker, J. P., Fukugita, M., & Cen, R. 2006, ApJ, 653, 881
Oke, J. B. 1990, AJ, 99, 1621
Pedichini, F., Giallongo, E., Ragazzoni, R., et al. 2003, Proc. SPIE, 4841, 815
Poli, F., Giallongo, E., Fontana, A., et al. 2003, ApJ, 593, L1
Radovich, M., Arnaboldi, M., Ripepi, V., et al., 2004, A&A, 417, 51
Ragazzoni, R., Giallongo, E., Pasian, F., et al. 2006, Proc. SPIE, 6267, 33
Sekiguchi, K., et al. 2004, Multiwavelength Cosmology. Proceedings of the Multiwavelength Cosmology conference, held on Mykonos Island, Greece, 17–20 June, 2003, ed. M. Plionis
Silva, L., Granato, G. L., Bressan, A., & Danese, L. 1998, ApJ, 509, 103
Somerville, R. S., Hopkins, P. F., Cox, T. J., et al. 2008, MNRAS, 391, 481
Speziali, R., Pedichini, F., Di Paola, A., et al. 2004, SPIE, 5492, 900
Speziali, R., Di Paola, A., Giallongo, E., et al. 2008, SPIE, 7014, 158
Springel, V., White, S. D. M., Jenkins, A., et al. 2005, Nature, 435, 629
Stanev, T., & Franceschini, A. 1998, ApJ, 494, L159
Steidel, C. C., Adelberger, K. L., Shapley, A. E., et al. 2003, ApJ, 592, 728
Trenti, M., & Stiavelli, M. 2008, ApJ, 676, 767
Totani, T., Yoshii, Y., Iwamuro, F., et al. 2001, ApJ, 550, L137
Viola, M., Monaco, P., Borgani, S., Murante, G., & Tornatore, L. 2008, MNRAS, 383, 777
Windhorst, R., Cohen, S., Jansen, R., et al. 2002, AAS, 201, 3207
Xu, C. K., Donas, J., Arnouts, S., et al. 2005, ApJ, 619, L11
Yan, H., & Windhorst, R. A. 2004, ApJ, 612, L93
Yasuda, N., Fukugita, M., Narayanan, V. K., et al. 2001, AJ, 122, 1104